DESY 95–167
hep-ph/9509abc
September 1995

Off shell W pair production in e^+e^- annihilation: The `CC11` process

D. Bardin [1,2] and T. Riemann [1]

[1] DESY – Zeuthen
Platanenallee 6, D-15738 Zeuthen, Germany

[2] Bogoliubov Laboratory for Theoretical Physics, JINR
ul. Joliot-Curie 6, RU-141980 Dubna, Moscow Region, Russia

ABSTRACT

The various four-fermion production channels in e^+e^- annihilation are discussed and the `CC11` process $e^+e^- \to \bar{f}_1^u f_1^d f_2^u \bar{f}_2^d$, $f \neq e$, is studied in detail. The cross section $d^2\sigma/ds_1 ds_2$, with s_1, s_2 being the invariant masses squared of the two fermion pairs, may be expressed by six generic functions. All but one may be found in the literature. The cross section, including initial state radiation and the Coulomb correction, is discussed and compared with other calculations from low energies up to $\sqrt{s} = 2$ TeV.

Email addresses: bardindy@cernvm.cern.ch, riemann@ifh.de

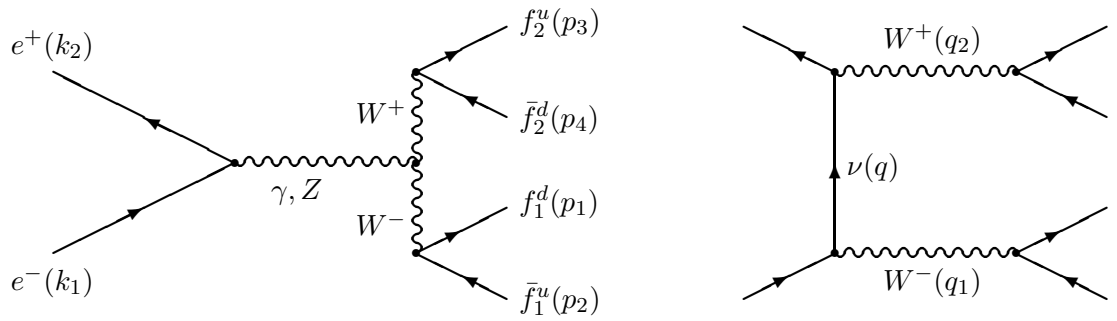

Figure 1: *The double resonating* `CC3` *contributions to off shell* W *pair production:* `crayfish` *and* `crab`*. They are part of all the processes of table 1.*

1 Introduction

A measurement of W pair production around and above the production threshold will be one of the main tasks of LEP 2 [1] as well as of a future high energy linear e^+e^- collider [2].

Immediately after their creation, the W bosons decay and four-fermion ($4f$) production is observed:

$$e^+e^- \to (W^-W^+) \to 4f. \tag{1.1}$$

This double resonating process proceeds via the diagrams shown in figure 1. In addition, there are a lot of Feynman diagrams with the same final state, but different intermediate states, which are single resonant or non-resonant and often called background diagrams. Their number and complexity vary in dependence on the composition of the final state. The total numbers of Feynman diagrams for the different channels are shown in table 1.

	$\bar{d}u$	$\bar{s}c$	$\bar{e}\nu_e$	$\bar{\mu}\nu_\mu$	$\bar{\tau}\nu_\tau$
$d\bar{u}$	*43*	**11**	20	**10**	**10**
$e\bar{\nu}_e$	20	20	*56*	18	18
$\mu\bar{\nu}_\mu$	**10**	**10**	18	*19*	**9**

Table 1: *Number of Feynman diagrams contributing to the production of two fermion doublets.*

One may distinguish three different event classes, all of them containing the `CC3` process[1]:

(i) The `CC11` process.
The two fermion pairs are different, the final state does not contain identical particles nor electrons or electron neutrinos (numbers in table 1 in **boldface**). The corresponding eleven diagrams are shown in figures 1 and 2. There are less diagrams if neutrinos are produced (`CC9, CC10` processes).

[1] In [3], a slightly different classification has been introduced; the relation of both schemes is discussed in [4].

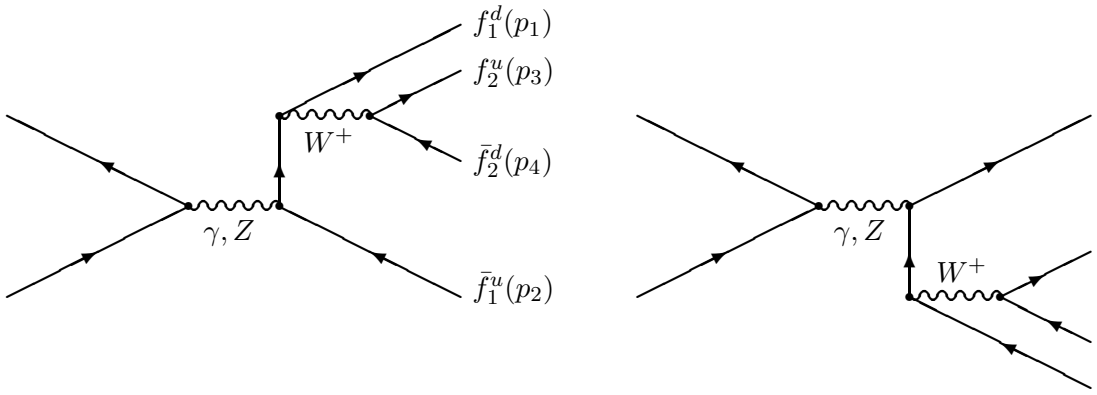

Figure 2: *Single resonant contributions to off shell W pair production: a u-*`deer` *and a d-*`deer`*.*

(ii) The `CC20` process.
The final state contains one $e^{\pm}$ together with its neutrino (Roman numbers in table 1); compared to case (i), the additional diagrams have a t channel gauge boson exchange. For a purely leptonic final state, a `CC18` process results.

(iii) The `mix43` and `mix56` processes.
Two mutually charge conjugated fermion pairs are produced (*italic* numbers in table 1). Differing from cases (i) and (ii), the diagrams may contain neutral boson exchanges[2] (see also table 2 in [5] where 'neutral current' type final states are classified). There are less diagrams in the `mix43` process if neutrinos are produced (`mix19` process).

In this article, we will investigate the simplest topology, case (i), which proceeds via the diagrams of figures 1 and 2:

$$e^+e^- \to \bar{f}_1^u f_1^d f_2^u \bar{f}_2^d, \qquad f_1 \neq f_2,\ f_i \neq e. \tag{1.2}$$

As far as *observable* final states are concerned, the following reactions are covered by this study:

(i) $(\bar{\mu}\nu_\mu) + (\tau\bar{\nu}_\tau)$;

(ii) $(l\bar{\nu}_l) + (q_u\bar{q}_d), \quad l = \mu, \tau$;

(iii) $(\bar{u}d) + (c\bar{s})$.

We parameterize the seven-dimensional four particle phase space as a sequence of two particle phase spaces:

$$\begin{aligned} d\Gamma &= \prod_{i=1}^{4} \frac{d^3p_i}{2p_i^0} \times \delta^4(k_1 + k_2 - \sum_{i=1}^{4} p_i) \\ &= \frac{\pi}{256} \frac{\sqrt{\lambda(s, s_1, s_2)}}{s} \frac{\sqrt{\lambda(s_1, m_1^2, m_2^2)}}{s_1} \frac{\sqrt{\lambda(s_2, m_3^2, m_4^2)}}{s_2} ds_1\, ds_2\, d\cos\theta\, d\Omega_1\, d\Omega_2, \end{aligned} \tag{1.3}$$

[2] We exclude the Higgs boson exchange diagrams from the discussion. In fact, the methods developed here are applicable also for the study of associated Higgs production [6].

with the usual definition of the λ function,

$$\begin{aligned} \lambda(a,b,c) &= a^2+b^2+c^2-2ab-2ac-2bc, & (1.4)\\ \lambda &\equiv \lambda(s,s_1,s_2). & (1.5) \end{aligned}$$

In (1.3), the rotation angle around the beam axis has been integrated over already. Variables k_1 and k_2 are the four-momenta of electron and positron and p_1, p_2, p_3, p_4 are those of the final state particles $f_1^d, \bar{f}_1^u, f_2^u, \bar{f}_2^d$ with $p_i^2 = m_i^2$ [3]. The invariant masses squared of the fermion pairs are:

$$\begin{aligned} s &= (k_1+k_2)^2, & (1.6)\\ s_1 &= (p_1+p_2)^2, & (1.7)\\ s_2 &= (p_3+p_4)^2. & (1.8) \end{aligned}$$

The W^- production angle θ in the center of mass system is spanned by the vectors $(\vec{p_1}+\vec{p_2})$ and $\vec{k}_1$. The spherical angle of $\vec{p_1}$ ($\vec{p_3}$) in the rest frame of the fermion pair $[f_1\bar{f}_1]$ ($[f_2\bar{f}_2]$) is Ω_1 (Ω_2): $d\Omega_i = d\cos\theta_i\, d\phi_i$. In this frame, the $\vec{p_2}$ ($\vec{p_4}$) points into the opposite direction with respect to $\vec{p_1}$ ($\vec{p_3}$) . The kinematical ranges of the integration variables are:

$$\begin{aligned} (m_1+m_2)^2 &\le s_1 \le (\sqrt{s}-m_3-m_4)^2, & (1.9)\\ (m_3+m_4)^2 &\le s_2 \le (\sqrt{s}-\sqrt{s_1})^2, & (1.10)\\ -1 &\le \cos\theta,\ \cos\theta_1,\ \cos\theta_2 \le 1, & (1.11)\\ 0 &\le \phi_1, \phi_2 \le 2\pi. & (1.12) \end{aligned}$$

We are interested in analytical formulae for distributions in invariant masses of fermion pairs. Thus, we have to integrate analytically over the five angular variables in (1.3). The squared matrix elements have been derived with `CompHEP` [7] and the angular integrations were performed with the aid of `FORM` [8].

The cross section contributions may be grouped into several classes of interferences:

$$\sigma_{\texttt{CC11}}(s) = \int ds_1 ds_2 \left[\sigma_{\texttt{CC3}} + \sigma^{3f} + \sigma^{\nu f} + \sigma^{ff} + \sigma^{f_1 f_2}\right]. \qquad (1.13)$$

In (1.13), the `CC3` process is accompanied by the interferences σ^{3f} of `deers` with the `crayfish` diagrams, the interferences $\sigma^{\nu f}$ of `deers` with the `crab`, the interferences σ^{ff} of `deers` of one doublet, and the interferences $\sigma^{f_1 f_2}$ of `deers` of different doublets.

Each of these contributions may be described by the product of a coefficient function $\mathcal{C}$, which is composed out of coupling constants and gauge boson propagators, and a kinematical function $\mathcal{G}(s, s_1, s_2)$. The latter depends only on the three invariant masses and contains the dynamics of the corresponding hard scattering process. The $\mathcal{G}$ functions, which are needed for a description of the `CC11` process are shown in table 4. The double resonating `CC3` process is known for long to be described by three kinematical functions [9]: $\mathcal{G}^a_{\texttt{CC3}}, a = 33, 3f, ff$. The double resonating neutral current `NC2` process, $e^+e^- \to (ZZ) \to 4f$, proceeds via two diagrams of the `crab` type and is characterized by only one kinematical function $\mathcal{G}_{\texttt{NC2}}$ [4] [10]. We

[3] Fermion masses are retained in the phase space definitions and in the basic kinematical relations. In all subsequent steps of the calculation, they will be neglected compared to invariants s, s_1, and s_2.

[4] Since not only Z pairs, but also $Z\gamma$ and $\gamma\gamma$ intermediate states exist one is faced in practice with an `NC8` process with the same topology like `NC2`.

also have to mention that the simplest final state configuration of a complete neutral current $4f$ process has 24 Feynman diagrams and requires, besides $\mathcal{G}_{\texttt{NC2}}$, only one additional function $\mathcal{G}_{\texttt{NC24}}$ [5]. It will be shown below that a complete description of the CC11 process after the angular integrations is possible with adding only one further function $\mathcal{G}^{u,d}_{\texttt{CC11}}$.

process	$\sigma_{\texttt{CC3}}$	σ^{3f}	$\sigma^{\nu f}$	σ^{ff}	$\sigma^{f_1 f_2}$
$\mathcal{G}(s;s_1,s_2)$	$\mathcal{G}^{33}_{\texttt{CC3}}$, $\mathcal{G}^{3f}_{\texttt{CC3}}$, $\mathcal{G}^{ff}_{\texttt{CC3}}$	$\mathcal{G}^{3f}_{\texttt{CC3}}$	$\mathcal{G}^{u,d}_{\texttt{CC11}}$; $\mathcal{G}_{\texttt{NC24}}$	$\mathcal{G}^{ff}_{\texttt{CC3}}$; $\mathcal{G}_{\texttt{NC2}}$	$\mathcal{G}^{u,d}_{\texttt{CC11}}$; $\mathcal{G}_{\texttt{NC24}}$

Table 2: *The complete set of kinematical functions describing the* CC11 *process.*

In the next section, notations and the formulae for the CC3 process are introduced. In section 3, the contributions from the background diagrams of figure 2 are presented. The photonic initial state and Coulomb corrections are added in section 4 and section 5 contains numerical results and a discussion. Several appendices are devoted to technical details of the calculation.

2 The CC3 process

2.1 The total cross section

The double resonating cross section is:

$$\sigma_{\texttt{CC3}}(s;s_1,s_2) = \frac{\sqrt{\lambda}}{\pi s^2}\Big[\mathcal{C}^{s}_{\texttt{CC3}}\mathcal{G}^{33}_{\texttt{CC3}}(s;s_1,s_2)+\mathcal{C}^{st}_{\texttt{CC3}}\mathcal{G}^{3f}_{\texttt{CC3}}(s;s_1,s_2)+\mathcal{C}^{t}_{\texttt{CC3}}\mathcal{G}^{ff}_{\texttt{CC3}}(s;s_1,s_2)\Big]. \tag{2.1}$$

The kinematical functions are known from [9]:

$$\mathcal{G}^{33}_{\texttt{CC3}}(s;s_1,s_2) = \frac{\lambda}{48}\left[\lambda+12\left(ss_1+s_1s_2+s_2s\right)\right], \tag{2.2}$$

$$\mathcal{G}^{3f}_{\texttt{CC3}}(s;s_1,s_2) = \frac{1}{48}\Big\{\left(s-s_1-s_2\right)\left[\lambda+12s(ss_1+s_1s_2+s_2s)\right] - 24\left[ss_1+s_1s_2+s_2s\right]s_1s_2\mathcal{L}(s;s_1,s_2)\Big\}, \tag{2.3}$$

$$\mathcal{G}^{ff}_{\texttt{CC3}}(s;s_1,s_2) = \frac{1}{48}\left[\lambda+12s(s_1+s_2)-48s_1s_2+24(s-s_1-s_2)s_1s_2\mathcal{L}(s;s_1,s_2)\right]. \tag{2.4}$$

In the superscript, the '3' indicates to the matrix element with a three gauge boson vertex and 'f' to the diagram with fermion propagator. The function $\mathcal{G}^{3f}_{\texttt{CC3}}$ has been slightly simplified compared to [4, 9]. The logarithm in (2.3) and (2.4) arises from the integration over the fermion propagator in the t channel (see appendix C):

$$\mathcal{L}(s;s_1,s_2)=\frac{1}{\sqrt{\lambda}}\,\ln\frac{s-s_1-s_2+\sqrt{\lambda}}{s-s_1-s_2-\sqrt{\lambda}}. \tag{2.5}$$

Some properties of λ and $\mathcal{L}$ are collected for the convenience of the reader in appendix A.

For the coefficient functions, we choose generic definitions. At first glance this seems to lead to artificially complicated constructions. At a later stage, however, the usefulness will become quite evident. We begin with

$$\mathcal{C}^t_{\texttt{CC3}} = \sum_{V_i,V_j,V_k,V_l=W} \mathcal{C}^{ijkl|ee}_{422}(E,s;F_1,s_1;F_2,s_2). \tag{2.6}$$

The coefficient $\mathcal{C}^{ijkl|ab}_{422}$ has been introduced for the neutral current NC2 process in eq. (11) of [5]; with a slight change of notion for the current presentation, it becomes:

$$\begin{aligned}\mathcal{C}^{ijkl|ab}_{422}(F_2,s_2;F_1,s_1;E,s) &= \frac{2}{(6\pi^2)^2}\,\Re e\frac{1}{D_{V_i}(s)D_{V_j}(s_1)D^*_{V_k}(s)D^*_{V_l}(s_1)} \\ &\times \Big[L(f_2^a,V_i)L(f_2^b,V_k)L(f_2^a,V_j)L(f_2^b,V_l) \\ &+ R(f_2^a,V_i)R(f_2^b,V_k)R(f_2^a,V_j)R(f_2^b,V_l)\Big]N_c(F_2) \\ &\times \left[L(F_1,V_j)L(F_1,V_l)+R(F_1,V_j)R(F_1,V_l)\right]N_c(F_1) \\ &\times \left[L(E,V_i)L(E,V_k)+R(E,V_i)R(E,V_k)\right]N_c(E). \end{aligned}\tag{2.7}$$

The labels E, F_1, F_2 denote the corresponding members of weak isodoublets. For the charged current, all left- and right-handed fermion couplings are equal:

$$L(e,W) \equiv L(E,W) = L(F_i,W) = \frac{g}{2\sqrt{2}}, \tag{2.8}$$

$$R(e,W) \equiv R(E,W) = R(F_i,W) = 0. \tag{2.9}$$

Below we will also need neutral current couplings where flavors will cause differences for the couplings.

The boson propagator is:

$$D_V(s) = s - M_V^2 + i\sqrt{s}\Gamma_V(s). \tag{2.10}$$

With these definitions and using the relation $G_\mu/\sqrt{2} = g^2/(8M_W^2)$, one easily verifies that

$$C^t_{\texttt{CC3}} = \frac{\left(G_\mu M_W^2\right)^2}{s_1 s_2}\rho(s_1)\rho(s_2), \tag{2.11}$$

where

$$\rho(s_i) = \frac{1}{\pi}\frac{\sqrt{s_i}\,\Gamma_W(s_i)}{|s_i - M_W^2 + i\sqrt{s_i}\,\Gamma_W(s_i)|^2} \times \mathrm{BR}(i), \tag{2.12}$$

and

$$\Gamma_W(s_i) = \sum_f \frac{G_\mu\, M_W^2}{6\pi\sqrt{2}}\sqrt{s_i}. \tag{2.13}$$

The off shell width $\Gamma_W(s_i)$ is used throughout this paper. It contains a sum over all open fermion decay channels f at energy $\sqrt{s_i}$, and $\mathrm{BR}(i)$ is the corresponding branching ratio. Equation (2.11) makes the presence of the two Breit-Wigner factors explicit. These are normalized such that $\lim_{\Gamma_V\to 0}\rho(s_i) = \delta(s_i - M_W^2)\times BR(i)$.

The other two coefficient functions are:

$$\begin{aligned}
\mathcal{C}^{s}_{\mathsf{CC3}} &= \sum_{i,j=\gamma,Z} \frac{2}{\left(6\pi^2\right)^2} \Re e \frac{1}{\left|D_W(s_1)\right|^2 \left|D_W(s_2)\right|^2 D_{V_i}(s) D^*_{V_j}(s)} \\
&\times\ g_3(V_i) g_3(V_j) L^2(F_1,W) L^2(F_2,W) N_c(F_1) N_c(F_2) \\
&\times\ \left[L(e,V_i)L(e,V_j) + R(e,V_i)R(e,V_j)\right] N_c(E), \qquad (2.14) \\
\mathcal{C}^{st}_{\mathsf{CC3}} &= \sum_{j=\gamma,Z;k=W} \mathcal{C}^{jk}_{223}(F_1,s_1;e,s;F_2,s_2), \qquad (2.15) \\
\mathcal{C}^{jk}_{223}(F_1,s_1;h,s_h;F,s_f) &= \frac{2}{\left(6\pi^2\right)^2} \Re e \frac{1}{\left|D_W(s_1)\right|^2 D^*_W(s_2) D^*_{V_j}(s) D_{V_k}(s_f)} \\
&\times\ L^2(F_1,W) g_3(V_j) L^2(F_2,W) L(h,V_k) N_c(F_1) N_c(F_2) \\
&\times\ \left[L(e,V_j)L(e,V_k) + R(e,V_j)R(e,V_k)\right] N_c(E), \qquad (2.16)
\end{aligned}$$

with

$$\begin{aligned}
L(f,\gamma) &= \frac{eQ_f g}{2}, & L(f,Z) &= \frac{e}{4 s_W c_W}\left(2I^f_3 - 2Q_f s^2_W\right), \\
R(f,\gamma) &= \frac{eQ_f g}{2}, & R(f,Z) &= \frac{e}{4 s_W c_W}\left(-2Q_f s^2_W\right), \qquad (2.17) \\
g_3(\gamma) &= g s_W, & g_3(Z) &= g c_W,
\end{aligned}$$

and $e = g s_W = \sqrt{4\pi\alpha}$, $Q_e = -1, I^e_3 = -\frac{1}{2}$.

2.2 The angular distribution

It is quite useful to know not only the invariant mass distributions and the total cross section, but in addition also the distribution in the production angle of one of the W bosons:

$$\begin{aligned}
\frac{d\sigma_{\mathsf{CC3}}}{d\cos\theta} &= \frac{\sqrt{\lambda}}{\pi s^2}\Big[\mathcal{C}^{s}_{\mathsf{CC3}} \mathcal{G}^{33}_{\mathsf{CC3}}(s;s_1,s_2;\cos\theta) \\
&\quad + \mathcal{C}^{st}_{\mathsf{CC3}} \mathcal{G}^{3f}_{\mathsf{CC3}}(s;s_1,s_2;\cos\theta) + \mathcal{C}^{t}_{\mathsf{CC3}} \mathcal{G}^{ff}_{\mathsf{CC3}}(s;s_1,s_2;\cos\theta)\Big], \qquad (2.18)
\end{aligned}$$

with

$$\begin{aligned}
\mathcal{G}^{33}_{\mathsf{CC3}}(s;s_1,s_2;\cos\theta) &= \frac{1}{8}\left[\lambda C_1 + 12 s_1 s_2 C_2\right], \qquad (2.19) \\
\mathcal{G}^{3f}_{\mathsf{CC3}}(s;s_1,s_2;\cos\theta) &= \frac{1}{8}\left[(s-s_1-s_2)C_1 - \frac{4 s_1 s_2 [s(s_1+s_2) - C_2]}{t_\nu}\right], \qquad (2.20) \\
\mathcal{G}^{ff}_{\mathsf{CC3}}(s;s_1,s_2;\cos\theta) &= \frac{1}{8}\left[C_1 + \frac{4 s_1 s_2 C_2}{t^2_\nu}\right], \qquad (2.21)
\end{aligned}$$

and

$$\begin{aligned}
C_1 &= 2s(s_1+s_2) + C_2, \qquad (2.22) \\
C_2 &= t_\nu(s - s_1 - s_2 - t_\nu) - s_1 s_2. \qquad (2.23)
\end{aligned}$$

The scattering angle is contained in the denominator of the t channel propagator:

$$t_\nu = \frac{1}{2}\left(s - s_1 - s_2 - \sqrt{\lambda}\cos\theta\right). \qquad (2.24)$$

With the aid of appendix C, it is trivial to integrate over $\cos\theta$:

$$\mathcal{G}^a_{\texttt{CC3}}(s,s_1,s_2) = \frac{1}{2}\int_{-1}^{1} d\cos\theta\ \mathcal{G}^a_{\texttt{CC3}}(s,s_1,s_2;\cos\theta), \qquad a = 33, 3f, ff. \tag{2.25}$$

The distribution (2.18) is used for the description of W pair production in `PYTHIA` [11]. It also may be used for the calculation of moments like

$$\int ds_1\, ds_2\, d\cos\theta\ \cos^n\theta\, \frac{d\sigma}{ds_1 ds_2 d\cos\theta} \tag{2.26}$$

as a check on the accuracy of Monte Carlo integrations [12]. The angular distribution is more interesting in the context of anomalous couplings of gauge bosons [13].

3 Background contributions

We now come to the contributions from the eight background diagrams of figure 2 and from their interferences with the double resonating diagrams of figure 1. For this purpose, we use a classification, which was introduced for neutral current processes in [5]. A single resonant diagram with a virtual fermion f is called an f-`deer`. Strictly speaking, the `deers` are double resonating diagrams as `crabs` are: besides the one W resonance, they contain the s channel Z (or γ) propagator. One of the invariant masses, in which the diagram may become resonating, is 'eaten' by the fermion line. In the `crab` it is s, while in a `deer` either s_1 or s_2. In this language, the `crab` is an e-`deer`. In appendix C it is made plausible that in fact this observation may be used for a treatment of all the contributions on an equal footing.

3.1 The `crayfish-deer` interferences σ^{3f}

The interferences of the `crayfish` diagram with the four types of `deers` are similar to the `crayfish-crab` interference:

$$\sigma^{3f} = \frac{\sqrt{\lambda}}{\pi s^2}\sum_{n=1,2}\left[\mathcal{C}^{3u_n}_{\texttt{CC11}} + \mathcal{C}^{3d_n}_{\texttt{CC11}}\right]\mathcal{G}^{3f}_{\texttt{CC3}}(s_n;s,s_{3-n}). \tag{3.1}$$

The coefficient function is

$$\mathcal{C}^{3f_n}_{\texttt{CC11}} = \sum_{V_j,V_k=\gamma,Z}\mathcal{C}^{jk}_{223}(F_{3-n},s_{3-n};f_n,s_n;e,s), \tag{3.2}$$

and $\mathcal{G}^{3f}_{\texttt{CC3}}$ is defined in (2.3) and $\mathcal{C}^{jk}_{223}$ in (2.16).

3.2 The `deer` interferences σ^{ff}

The contribution from the square of two `deers`, which belong to one doublet $F = (f^u, f^d)$ occurs twice:

$$\sigma^{ff} = \frac{\sqrt{\lambda}}{\pi s^2}\sum_{n=1,2}\left\{\left[\mathcal{C}^{f^u_n f^u}_{\texttt{CC11}} + \mathcal{C}^{f^d_n f^d}_{\texttt{CC11}}\right]\mathcal{G}^{ff}_{\texttt{CC3}}(s_n;s_{3-n},s) + \mathcal{C}^{f^u_n f^d}_{\texttt{CC11}}\ \mathcal{G}^{u,d}_{\texttt{CC11}}(s_n;s_{3-n},s)\right\}, \tag{3.3}$$

with the coefficient function

$$\mathcal{C}^{f_n^a f_n^b}_{\texttt{CC11}} = \sum_{V_i,V_k=\gamma,Z|V_j=V_l=W} \mathcal{C}^{ijkl|ab}_{422}(F_n,s_n;F_m,s_m;E,s). \tag{3.4}$$

The $\mathcal{C}^{ijkl|ab}_{422}$ is defined in (2.7).

The kinematical functions are different for the pure squares of diagrams, where (2.4) is to be used, and for their interference. The latter may be expressed by known functions. Let us refer for a moment to the neutral current case. There, all couplings are equal and one gets the following relation: $\mathcal{G}_{\texttt{NC2}} = \mathcal{G}^{uu} + \mathcal{G}^{dd} + \mathcal{G}^{ud}$. With $\mathcal{G}^{uu} = \mathcal{G}^{dd} = \mathcal{G}^{ff}_{\texttt{CC3}}$, and $\mathcal{G}^{ud} = \mathcal{G}^{ud}_{\texttt{CC11}}$, one gets the requested identity,

$$\mathcal{G}^{ud}_{\texttt{CC11}}(s;s_1,s_2) = \mathcal{G}_{\texttt{NC2}}(s;s_1,s_2) - 2\,\mathcal{G}^{ff}_{\texttt{CC3}}(s;s_1,s_2), \tag{3.5}$$

with the neutral current function $\mathcal{G}_{\texttt{NC2}}$ from [10]; see appendix D.

3.3 The `deer` interferences $\sigma^{f_1 f_2}$

There are four interferences among `deer` diagrams belonging to different doublets:

$$\sigma^{f_1 f_2} = \frac{\sqrt{\lambda}}{\pi s^2}\Big\{\left[\mathcal{C}^{f_1^u f_2^u} + \mathcal{C}^{f_1^d f_2^d}\right]\mathcal{G}^{uu,dd}_{\texttt{CC11}}(s;s_1,s_2) + \left[\mathcal{C}^{f_1^u f_2^d} + \mathcal{C}^{f_1^d f_2^u}\right]\mathcal{G}^{u,d}_{\texttt{CC11}}(s;s_1,s_2)\Big\}. \tag{3.6}$$

The coefficient function may be traced back to that introduced in [5]:

$$\mathcal{C}^{f_1^a f_2^b} = \sum_{V_i,V_k=\gamma,Z|V_j,V_l=W} \mathcal{C}^{ijkl}_{233}(E,s;f_1^a,s_1;f_2^b,s_2). \tag{3.7}$$

The function $\mathcal{C}^{ijkl}_{233}$ is defined as follows:

$$\begin{aligned}\mathcal{C}^{ijkl}_{233}(E,s;F_1,s_1;F_2,s_2) &= \frac{2}{(6\pi^2)^2}\,\Re e\frac{1}{D_{V_i}(s)D^*_{V_k}(s)D_{V_l}(s_1)D^*_{V_j}(s_2)}\\ &\times\ [L(E,V_i)L(E,V_k) + R(E,V_i)R(E,V_k)]\,N_c(E)\\ &\times\ [L(F_1,V_l)L(F_1,V_j)L(F_1,V_k) - R(F_1,V_l)R(F_1,V_j)R(F_1,V_k)]\,N_c(F_1)\\ &\times\ [L(F_2,V_l)L(F_2,V_j)L(F_2,V_i) - R(F_2,V_l)R(F_2,V_j)R(F_2,V_i)]\,N_c(F_2).\end{aligned} \tag{3.8}$$

Wherever a neutral gauge boson couples, the corresponding fermion e or f_2 etc. will replace the doublets E, F_2 in the arguments of the couplings L, R.

For the kinematical functions, again a relation to a neutral current function may be established. The function $\mathcal{G}_{\texttt{NC24}}$, explicitly given in appendix D, describes a sum of interferences analogue to those considered here. Since the couplings are equal in that case, we have: $\mathcal{G}_{\texttt{NC24}} = \mathcal{G}^{u_1u_2} + \mathcal{G}^{u_1d_2} + \mathcal{G}^{d_1u_2} + \mathcal{G}^{d_1d_2}$. Furthermore, using the symmetry relations $\mathcal{G}^{u_1u_2} = \mathcal{G}^{d_1d_2} \equiv \mathcal{G}^{uu,dd}_{\texttt{CC11}}$ and $\mathcal{G}^{u_1d_2} = \mathcal{G}^{d_1u_2} \equiv \mathcal{G}^{u,d}_{\texttt{CC11}}$, we may write $\mathcal{G}_{\texttt{NC24}} = 2\mathcal{G}^{uu,dd}_{\texttt{CC11}} + 2\mathcal{G}^{u,d}_{\texttt{CC11}}$. This relation allows to determine $\mathcal{G}^{uu,dd}_{\texttt{CC11}}$ once $\mathcal{G}^{u,d}_{\texttt{CC11}}$ is known:

$$\mathcal{G}^{uu,dd}_{\texttt{CC11}} = \frac{1}{2}\mathcal{G}_{\texttt{NC24}} - \mathcal{G}^{u,d}_{\texttt{CC11}}. \tag{3.9}$$

By an explicit calculation, we obtained:

$$\begin{aligned}
\mathcal{G}^{u,d}_{\texttt{CC11}}(s;s_1;s_2) = &-120s^4\frac{s_1^3s_2^3}{\lambda^3}\mathcal{L}(s_2;s,s_1)\mathcal{L}(s_1;s_2,s)\\
&-s\left[1+\frac{s(s-\sigma)}{\lambda}+20s^2\frac{s_1s_2}{\lambda^2}-30s^3s_1s_2\frac{s-3\sigma}{\lambda^3}\right]\left[s_1^2\mathcal{L}(s_2;s,s_1)+s_2^2\mathcal{L}(s_1;s_2,s)\right]\\
&-s(s_1-s_2)\left[\frac{s-\sigma}{\lambda}+10s\frac{s_1s_2}{\lambda^2}-30s^2s_1s_2\frac{s+\sigma}{\lambda^3}\right]\left[s_1^2\mathcal{L}(s_2;s,s_1)-s_2^2\mathcal{L}(s_1;s_2,s)\right]\\
&-\frac{1}{12}\Bigg\{(s^2-\sigma^2)\left[1+12\frac{s\sigma}{\lambda}-60s^2\frac{s_1s_2}{\lambda^2}\right]\\
&\qquad -8s_1s_2\left[1-\frac{s(4s+5\sigma)}{\lambda}+15s^2\frac{s_1s_2}{\lambda^2}\left(1-6\frac{s(s-\sigma)}{\lambda}\right)\right]\Bigg\},
\end{aligned} \tag{3.10}$$

where $\sigma = s_1 + s_2$.

For numerical applications, it is helpful to know the limit $\lambda \to 0$:

$$\lim_{\lambda\to 0}\mathcal{G}^{u,d}_{\texttt{CC11}}(s;s_1;s_2) \;=\; -\frac{1}{64}\left(s^2-\Delta^2\right)\left(9-\frac{\Delta^2}{s^2}\right)+\frac{\lambda}{160}\left(1+9\frac{\Delta^2}{s^2}\right)+\mathcal{O}(\lambda^2), \tag{3.11}$$

where $\Delta = s_1 - s_2$.

3.4 The `crab-deer` interferences $\sigma^{\nu f}$

There are four `crab-deer` interferences:

$$\sigma^{\nu f} \;=\; \frac{\sqrt{\lambda}}{\pi s^2}\sum_{n=1,2}\left[\mathcal{C}^{\nu_e u_n}_{\texttt{CC11}}\;\mathcal{G}^{u,d}_{\texttt{CC11}}(s_{3-n};s,s_n)+\mathcal{C}^{\nu_e d_n}_{\texttt{CC11}}\;\mathcal{G}^{uu,dd}_{\texttt{CC11}}(s_{3-n};s,s_n)\right]. \tag{3.12}$$

The coefficient functions are:

$$\mathcal{C}^{\nu_e f_n}_{\texttt{CC11}} \;=\; \sum_{V_i=\gamma,Z|V_j,V_k,V_l=W}\mathcal{C}^{ljki}_{233}(F_{3-n},s_{3-n};E,s,f_n,s_n), \tag{3.13}$$

and the $\mathcal{C}^{ljki}_{233}$ is defined in (3.8).

The kinematical functions are introduced in section 3.3. One should be aware of a factor $\frac{1}{2}$ resulting in the limit of neutral couplings. Differing from the neutral current case, there is no charged current crossed `crab` diagram, which would give the same contribution as the `crab` diagram.

4 QED corrections

A complete treatment of QED corrections for four-fermion production is part of electroweak corrections and a quite ambitious task [14]. For the time being, one may try to restrict to initial state radiation (ISR) and, near the W pair production threshold, corrections from the Coulomb singularity. Both corrections influence the cross section significantly.

4.1 Flux function approach

The cross section with QED corrections becomes in the flux function approach:

$$\frac{d\sigma_{QED}(s)}{ds_1 ds_2} = \int\limits_{(\sqrt{s_1}+\sqrt{s_2})^2}^{s} \frac{ds'}{s}\Big\{G(s'/s)\Big[\sigma_{\texttt{CC11}}(s',s_1,s_2) + C(s')\sigma_{\texttt{CC3}}(s',s_1,s_2)\Big] + \sigma_{QED}^{non-univ}(s',s_1,s_2)\Big\}, \tag{4.1}$$

with

$$G(s'/s) = \beta_e\left(1-\frac{s'}{s}\right)^{\beta_e-1}(1+S) + H(s',s), \tag{4.2}$$

and

$$\beta_e = \frac{2\alpha}{\pi}\left(L_e - 1\right), \tag{4.3}$$

$$L_e = \ln\frac{s}{m_e^2}. \tag{4.4}$$

The virtual and soft corrections S and hard corrections H are [15]:

$$S = \frac{3}{4}\beta_e + \frac{\alpha}{\pi}\left(\frac{\pi^2}{3}-\frac{1}{2}\right)\times \texttt{IZERO} + S^{(2)}, \tag{4.5}$$

$$S^{(2)} = \left(\frac{\alpha}{\pi}\right)^2\Big[s_2 L_e^2 + s_1 L_e + s_0\Big] + S^{(2)}_{pairs}, \tag{4.6}$$

$$H(s',s) = -\frac{1}{2}\left(1+\frac{s'}{s}\right)\beta_e + H^{(2)}, \tag{4.7}$$

$$H^{(2)} = \left(\frac{\alpha}{\pi}\right)^2\Big[h_2 L_e^2 + h_1 L_e + h_0\Big] + H^{(2)}_{pairs}, \tag{4.8}$$

where the corrections $S^{(2)}_{pairs}$ and $H^{(2)}_{pairs}$ due to fermion pair emission from the initial state have been determined in [16].

In the leading logarithmic approximation (LLA), the ISR is well defined. The complete $\mathcal{O}(\alpha)$ corrections include additional contributions in case of t channel exchanges. They have been defined and determined for the double resonating `CC3` ([17]) and `NC2` ([18]) processes. For a complete treatment of the `CC11` process, this is not sufficient and has to be accomplished by a proper treatment of the `crayfish-deer` interferences; these are, however, small and the non-leading QED corrections to them the more.

The Coulomb corrections apply to the double resonating diagrams [19]:

$$C(s) = \frac{\alpha(2M_W)}{\beta}\,\Im m\ln\left[\frac{\beta_W+\delta-\beta}{\beta_W+\delta+\beta}\right], \tag{4.9}$$

$$\beta = \frac{1}{s}\sqrt{\lambda}, \tag{4.10}$$

$$\beta_W = \frac{1}{s}\sqrt{\lambda\left(s,m_W^2,m_W^2\right)}, \tag{4.11}$$

$$m_W^2 = M_W^2 - iM_W\Gamma_W, \tag{4.12}$$

$$\delta = \frac{1}{s}\left|s_1^2 - s_2^2\right|. \tag{4.13}$$

Besides the cross section, there is also experimental interest to know the radiative energy loss due to ISR. This quantity cannot be calculated in the flux function approach. However, the calculation of a similar quantity, namely the invariant mass loss (of final state fermions) is possible:

$$\langle m_\gamma \rangle \;=\; \frac{1}{\sigma}\int ds_1 ds_2 \int \frac{ds'}{s}\frac{\sqrt{s}}{2}\left(1-\frac{s'}{s}\right)\frac{d\sigma}{ds_1 ds_2 ds'}, \tag{4.14}$$

where $d\sigma/ds_1 ds_2 ds'$ is the contents of the curly brackets in (4.1).

4.2 Structure function approach

Alternatively, the structure function approach may be realized with the following formula:

$$\begin{aligned}\frac{d\sigma_{QED}(s)}{ds_1 ds_2} \;=\; &\int\limits_{x_1^{\min}}^{1} dx_1 \int\limits_{x_2^{\min}}^{1} dx_2\, D(x_1,s)D(x_2,s)\Big\{\sigma_{\texttt{CC11}}(x_1x_2s,s_1,s_2)\\ &+ C(x_1x_2s)\sigma_{\texttt{CC3}}(x_1x_2s,s_1,s_2)\Big\}.\end{aligned} \tag{4.15}$$

The lower integration boundaries are:

$$x_1^{\min} \;=\; \frac{(\sqrt{s_1}+\sqrt{s_2})^2}{s}, \tag{4.16}$$

$$x_2^{\min} \;=\; \frac{(\sqrt{s_1}+\sqrt{s_2})^2}{x_1 s}. \tag{4.17}$$

To a very good accuracy, the structure function may be written as follows [20]:

$$D(x,s) \;=\; (1-x)^{\beta_e/2-1}\,\frac{\beta_e}{2}(1+S)+H(x,s), \tag{4.18}$$

and

$$S \;=\; \frac{e^{(3/4-\gamma_E)\beta_e/2}}{\Gamma\left(1+\frac{\beta_e}{2}\right)}-1, \tag{4.19}$$

$$\begin{aligned}H(x,s) \;=\; &-\frac{1}{2}(1+x)\frac{\eta_e}{2}\\ &+\frac{1}{8}\left[-4(1+x)\ln(1-x)+3(1+x)\ln x-4\frac{\ln x}{1-x}-5-x\right]\left(\frac{\eta_e}{2}\right)^2,\end{aligned} \tag{4.20}$$

$$\eta_e \;=\; \frac{2\alpha}{\pi}\left(L_e-\texttt{IZETTA}\right). \tag{4.21}$$

Within a given order of LLA, the structure function and the flux function approaches are related:

$$G(s'/s) \;=\; \int dx_1 dx_2\, D(x_1,s)D(x_2,s)\,\delta\left(x_1x_2-\frac{s'}{s}\right). \tag{4.22}$$

The radiative energy loss is determined as follows:

$$\langle E_\gamma \rangle \;=\; \frac{1}{\sigma}\int ds_1 ds_2 \int dx_1 dx_2\, D(x_1,s)D(x_2,s)\frac{\sqrt{s}}{2}[(1-x_1)+(1-x_2)]\frac{d\sigma}{ds_1 ds_2 dx_1 dx_2}, \tag{4.23}$$

and the invariant mass loss (of final state fermions) is:

$$\langle m_\gamma \rangle \;=\; \frac{1}{\sigma}\int ds_1 ds_2 \int dx_1 dx_2\, D(x_1,s)D(x_2,s)\frac{\sqrt{s}}{2}(1-x_1x_2)\frac{d\sigma}{ds_1 ds_2 dx_1 dx_2}, \tag{4.24}$$

where $d\sigma/ds_1 ds_2 dx_1 dx_2$ is the content of the curly bracket in (4.15).

In table 3, we have collected the flags, which are used in `GENTLE` in order to define the details of the calculations.

Flag	FF	SF		
`ICONVL`	0	1		
`ICOLMB`	0 – 5	–	3	0
`IQEDHS`	0 – 4	–	3	2
`IZERO`	0, 1	–	1	0
`IZETTA`	–	0, 1	1	1
`ITVIRT`	0, 1	–	1	0
`ITBREM`	0, 1	–	1	0

Table 3: *Some of the flag settings in* `GENTLE` *for the flux function (FF) and the structure function (SF) approaches. The third column of flags contains recommended flag values for best estimates and the last one those chosen for the comparisons in table 6.*

5 Numerical results and discussion

The numerical results are obtained with the Fortran program `GENTLE` [21]. The input quantities are chosen as follows:

$$\begin{aligned} G_\mu &= 1.16639\times 10^{-5}\ \mathrm{GeV}^2, \\ \alpha(2M_W) &= (128.07)^{-1}, \\ M_Z &= 91.1888\ \mathrm{GeV}, \\ M_W &= 80.23\ \mathrm{GeV}. \end{aligned} \tag{5.1}$$

Further, for the QED corrections,

$$\alpha \;=\; (137.03599)^{-1}. \tag{5.2}$$

The s dependent widths are $\Gamma_V(s) = (\sqrt{s}/M_V)\Gamma_V$. For the Z width we use the value

$$\Gamma_Z = 2.4974\ \mathrm{GeV}, \tag{5.3}$$

thus circumventing a dependence of all the numbers on the top quark mass from a prediction of Γ_Z in the Standard Model [22]. For the W width the radiative corrections are small [23] and the following approximation is used:

$$\Gamma_W = 9 \times \frac{G_\mu M_W^3}{6\pi\sqrt{2}}. \tag{5.4}$$

Finally, we need the weak mixing angle $\sin^2\theta_W$. Again, we deviate from the pure Standard Model relation and use instead an effective weak mixing angle:

$$s_W^2 = \frac{\pi\alpha(2M_W)}{\sqrt{2}M_W^2 G_\mu}. \tag{5.5}$$

In table 5, cross section predictions are shown for the different channels of table 4 over a large range of $\sqrt{s}$. They are normalized by taking off the branching factors. The differences between the channels are seen to be minor above $\sqrt{s} \sim 160$ GeV, where the double resonating `CC3` diagram are dominating. Nevertheless, the predictions for the `CC3` process and any of the `CC11` processes start to deviate substantially above $\sqrt{s} = 200$ GeV.

$d_1\bar{u}_1$	$\bar{d}_2 u_2$	BR(1)×BR(2)
$l\nu$	$l\nu$	1/81
$l\nu$	$q^d q^u$	1/27
$q^d q^u$	$l\nu$	1/27
$q^d q^u$	$q^d q^u$	1/9
all	all	1

Table 4: *The branching ratios of the different types of final states of the* `CC11` *process.*

$\sqrt{s}$	`CC3`	$L\nu l\nu'$	$l\nu qq'$	$QQ'qq'$	`CC11`
30	1.4519×10^{-7}	5.9295×10^{-6}	7.2478×10^{-6}	5.0897×10^{-6}	6.1422×10^{-6}
60	1.9358×10^{-5}	4.0025×10^{-5}	4.6879×10^{-5}	3.5441×10^{-5}	4.1034×10^{-5}
91.189	0.11225	0.021329	0.024551	0.018975	0.021715
176	16.225	16.242	16.243	16.243	16.243
200	18.578	18.586	18.588	18.588	18.588
500	7.3731	7.3301	7.3318	7.3334	7.3323
1000	2.9888	2.9342	2.9344	2.9348	2.9347
2000	1.5702	1.5020	1.5018	1.5016	1.5017

Table 5: *Total cross sections in nbarn for the different Born 4f production channels as functions of $\sqrt{s}$ (in GeV). For this comparison, the branching ratios of table 4 are* not *taken into account in the single mode channels.*

Tables 6 and 7 compare for LEP 2 and table 8 for linear collider (LC) energies the numerical predictions of GENTLE with those of the Monte Carlo programs WPHACT [24], WWGENPV [25] and WTO [26]; the latter performs the numerical integrations with a deterministic approach. GENTLE may be used with both the flux function (FF) and the structure function (SF) approaches, while the other programs are based on the structure function approach. Shown are σ_{Born}, σ_{QED}, $\langle E_\gamma \rangle$, and $\langle m_\gamma \rangle$ as being introduced in section 4. For the observables with QED corrections, the first two lines at each energy show that both treatments of QED corrections agree well. Further, the predictions of the different programs are in perfect agreement with each other. Having in mind that some numbers arise from ninefold numerical integrations, this is a nontrivial result proving the high level of technical precision reached by now with quite different techniques. The dependence of cross sections on the channels has with QED corrections the same tendencies as in the Born case. As an example for this we mention that $\langle m_\gamma \rangle$ in table 7 shows, within the digits shown, no channel dependence at all.

	$\sqrt{s}$	176	190	205
σ_{Born}	GENTLE	1.8048	2.0405	2.0573
	WPHACT	1.8048(1)	2.0405(1)	2.0574(1)
	WWGENPV	1.8048(1)	2.0405(1)	2.0574(1)
σ_{QED}	GENTLE,FF	1.5067	1.8148	1.9022
	GENTLE,SF	1.5046	1.8124	1.8998
	WPHACT	1.5046(1)	1.8124(1)	1.8999(1)
	WTO	1.5046(1)	1.8124(3)	1.8996(4)
	WWGENPV	1.5045(1)	1.8124(1)	1.9000(1)

Table 6: *Results from different programs for the total* CC11 *cross sections* $e^+e^- \to 4f$ *and* $e^+e^- \to 4f + \gamma$ *(both in nbarn) at LEP 2 energies for the* $QQ'qq'$ *channel. The MC error estimates are indicated.*

	$\sqrt{s}$	176	190	205
$\langle E_\gamma \rangle$	GENTLE,SF	1.1151	2.1400	3.2025
	WPHACT	1.1149(2)	2.1402(4)	3.2030(6)
	WTO	1.1149(3)	2.1404(5)	3.2023(8)
	WWGENPV	1.1147(4)	2.1400(5)	3.2028(10)
$\langle m_\gamma \rangle$	GENTLE,FF	1.1129	2.1310	3.1816
	WWGENPV	1.1124(3)	2.1316(5)	3.1861(11)

Table 7: *Results from different programs for the average energy loss* $\langle E_\gamma \rangle$ *and the invariant mass loss* $\langle m_\gamma \rangle$ *(both in GeV) due to QED radiative corrections at LEP 2 energies in the* $l\nu\, qq'$ *channel.*

	$\sqrt{s}$	500	1000	2000
σ_{Born}	GENTLE	0.81482	0.32609	0.16684
	WWGENPV	0.81480(6)	0.32602(6)	0.16682(7)
σ_{QED}	GENTLE,SF	0.86950	0.36514	0.18247
	WPHACT	0.86956(9)	0.36515(5)	0.18250(4)
	WTO	0.86960(25)		
	WWGENPV	0.86956(14)	0.36530(35)	0.18247(13)

Table 8: *Results from different programs for the total* CC11 *cross sections* $e^+e^- \to 4f$ *and* $e^+e^- \to 4f + \gamma$ *(both in nbarn) at Linear Collider energies for the* $QQ'\,qq'$ *channel. The MC error estimates are indicated.*

Figure 3 shows, over a large energy range, the CC3 process without and with QED corrections. The latter smear out the W pair production peak and produce a radiative tail at higher energies, crossing over the Born curve at $\sqrt{s} \sim 240$ GeV. The Z resonance in the crayfish diagram leads to an interference pattern around $\sqrt{s} \sim 91$ GeV, with a set-on of the Z radiative tail until the W pair production starts to over-compensate it and to completely dominate the process.

The same, but now for the CC11 process, is shown in figure 4. As to be expected, the differences to the foregoing figure are not pronounced, although visible. Both the Z and W pair peaks (seen in the set-in as minima in $\sigma_{QED}/\sigma_{Born}$) are nearly untouched, while the tail of the Z between the two minima gets suppressed due to the background.

Direct comparisons of the CC3 and CC11 processes are shown in figure 5 without and in figure 6 with QED corrections. Quantitatively, the figures again do not differ too much. At the W pair production peak, the background influence is smallest, tending to negative contributions of few percents at large energies. Below the W pair production threshold, the CC3 process becomes heavily suppressed and background becomes equally important if not dominant.

5.1 Conclusions

We determined the so-called background contributions to the off shell W pair production cross section for the simplest final state configuration. Exploiting the inherent symmetries, we arrived at a remarkably compact presentation for the double differential distribution in the invariant masses of the W bosons. With no doubt, the angular distribution in the W production angle is also quite compact, as our expressions for the CC3 case indicate. Other angular distributions might be accessible as well; for the neutral current case, there are encouraging indications for that [27]. Staying more differential could be welcome to colleagues who search for anomalous gauge boson couplings, while, on the other hand, the advantages of the semi-analytical approach are partly lost. Anyhow, we see no principal problems arising when anomalous couplings are included. A step in this direction has been done for the CC3 process [28].

Finally, we would like to comment on the prospects of applications of our techniques to other four-fermion final state topologies. For the production of four untagged hadronic jets, one has to add incoherently the $qqgg$ final state, which should be straightforward. More

involved is the treatment of production of identical particles and/or of processes with gauge boson exchanges in the t channel. The first problem is due to permutations of final fermions in some of the diagrams, the second one by angular dependent gauge boson propagators, which occurs in e.g. the `CC20` process and is related to gauge invariance violation [29].

Time will show to what extent the technical obstacles mentioned will be overcome in the semi-analytical approach advocated here.

Acknowledgments

We would like to thank the MPI Munich for the kind hospitality extended to us in 1992 when this project was started. Together with M. Bilenky, we derived analytical results and, also with the aid of A. Olchevski, numerically reliable Fortran codes for the process `CC11` [4, 30]. At that time, the expressions for the kinematical functions $\mathcal{G}$ filled several pages. In 1994, A. Leike discovered nice symmetries for the process `NC24`. Guided by this, we found extreme simplifications for the process `CC11`. M.B. left the project before this level of understanding was reached. We acknowledge the contributions he made while he was joining us. Numerous numerical comparisons with results from Monte Carlo and deterministic approaches were very helpful. These were undertaken with A. Ballestrero, F. Berends, G. Montagna, O. Nicrosini, R. Pittau, G. Passarino, and F. Piccinini. Further, we would like to thank B. Kniehl, H. Kühn, D. Lehner, A. Leike, A. Olchevski, T. Sjostrand for discussions and valuable hints. D.B. is grateful to the Theoretical Physics Division of CERN and T.R. to the Aspen Center for Physics for the kind hospitality.

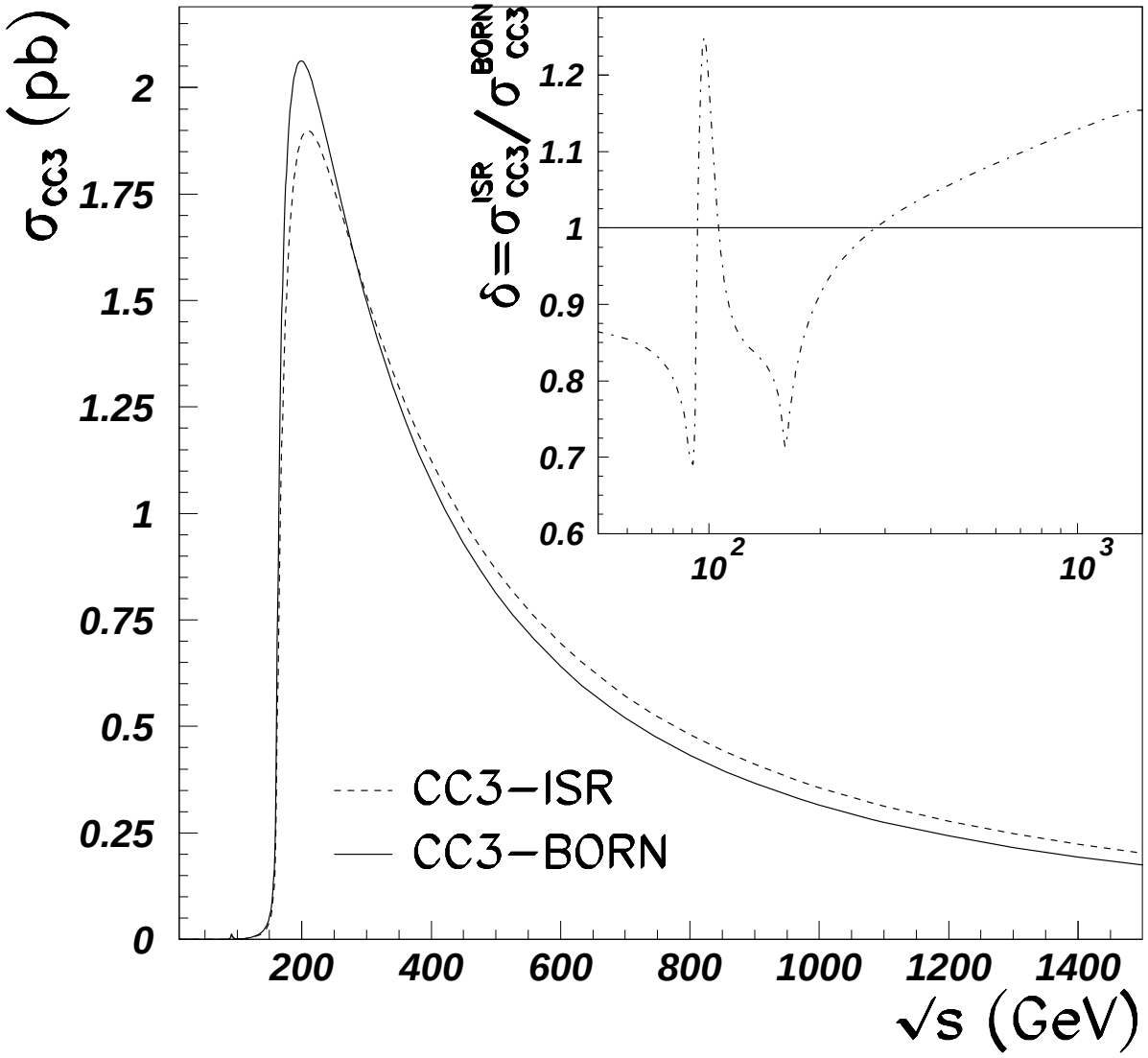

Figure 3: *The* CC3 *process without and with QED corrections.*

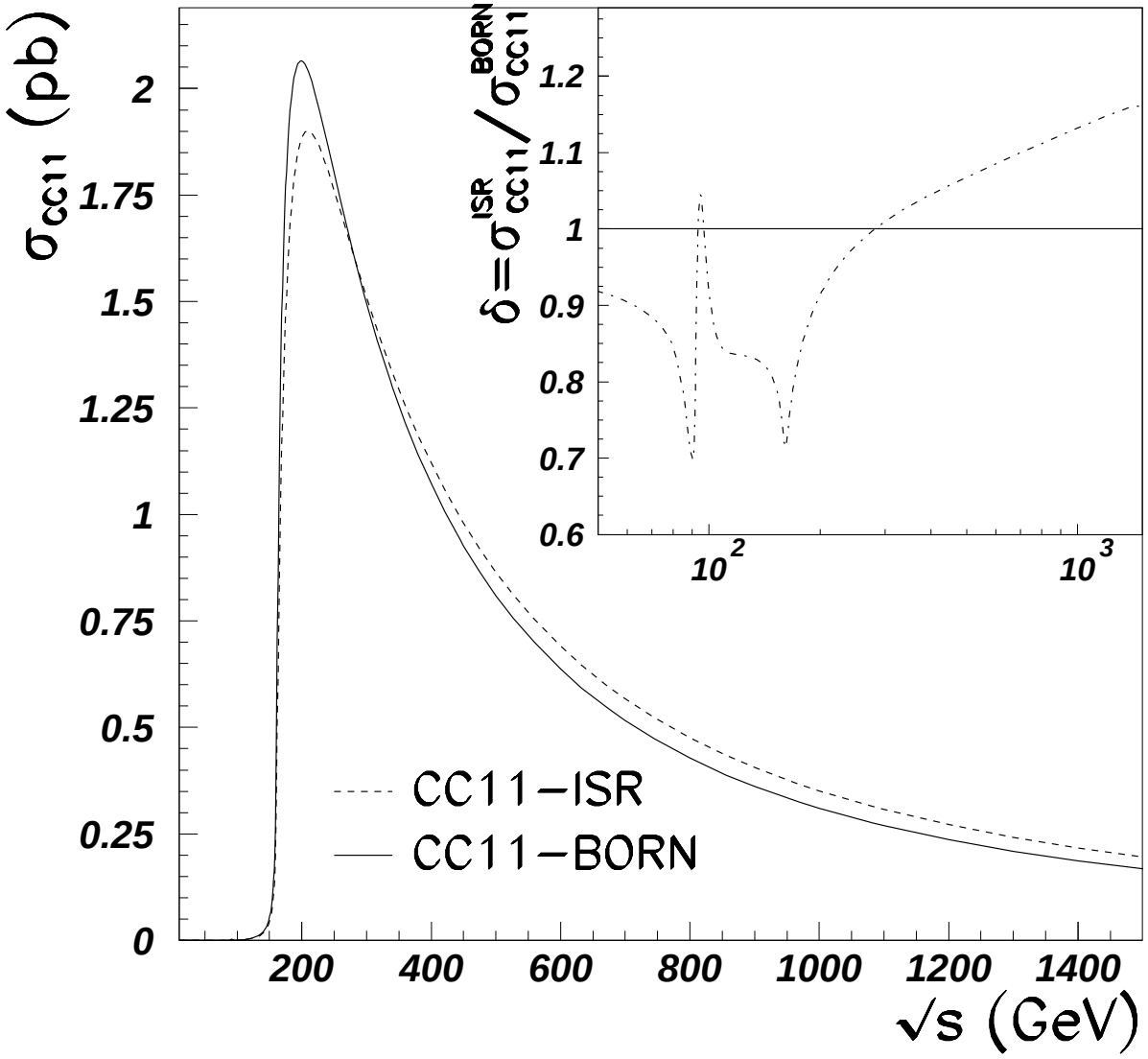

Figure 4: *The* `CC11` *process without and with QED corrections.*

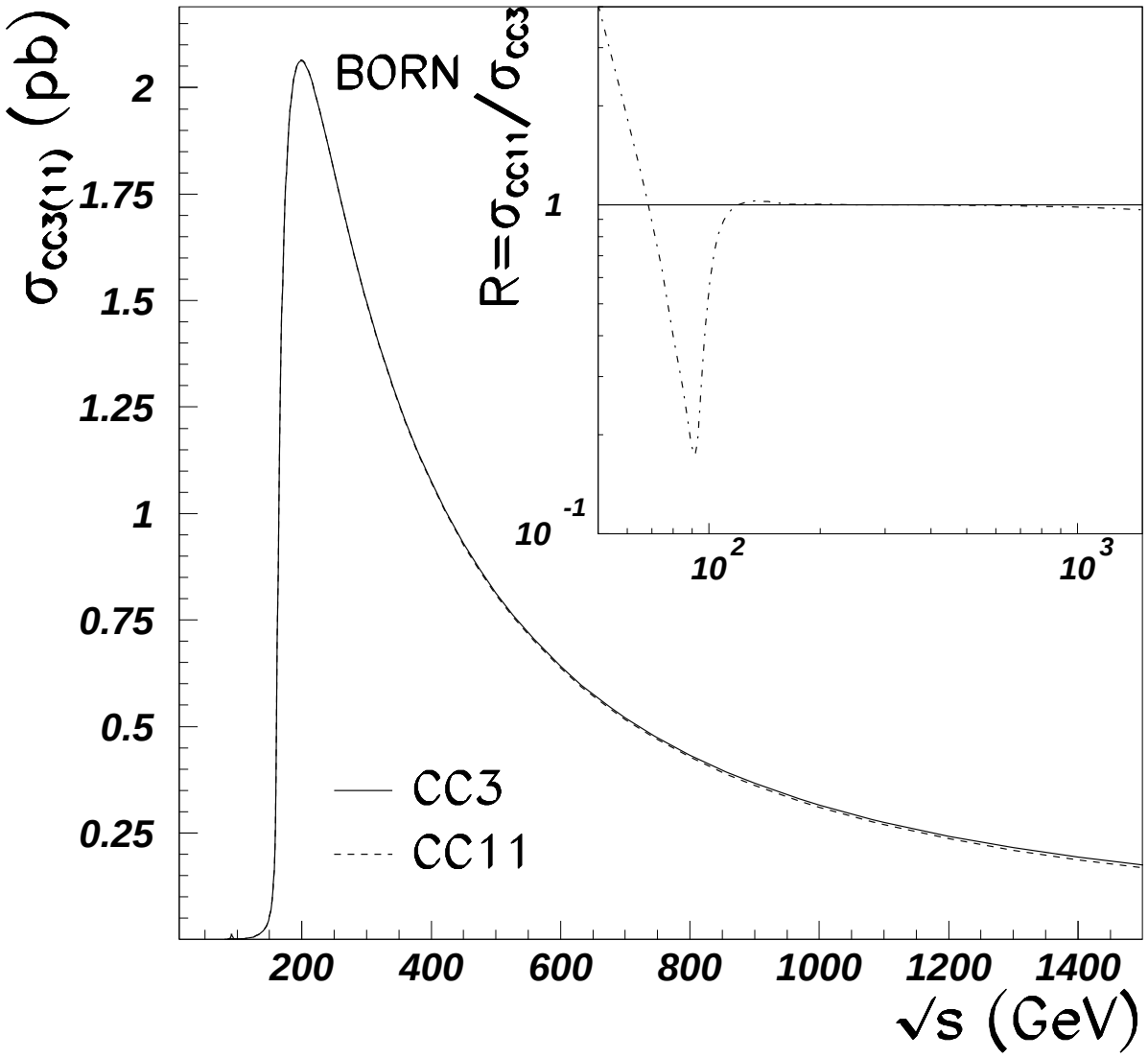

Figure 5: *The ratio of* `CC11` *and* `CC3` *processes without QED corrections.*

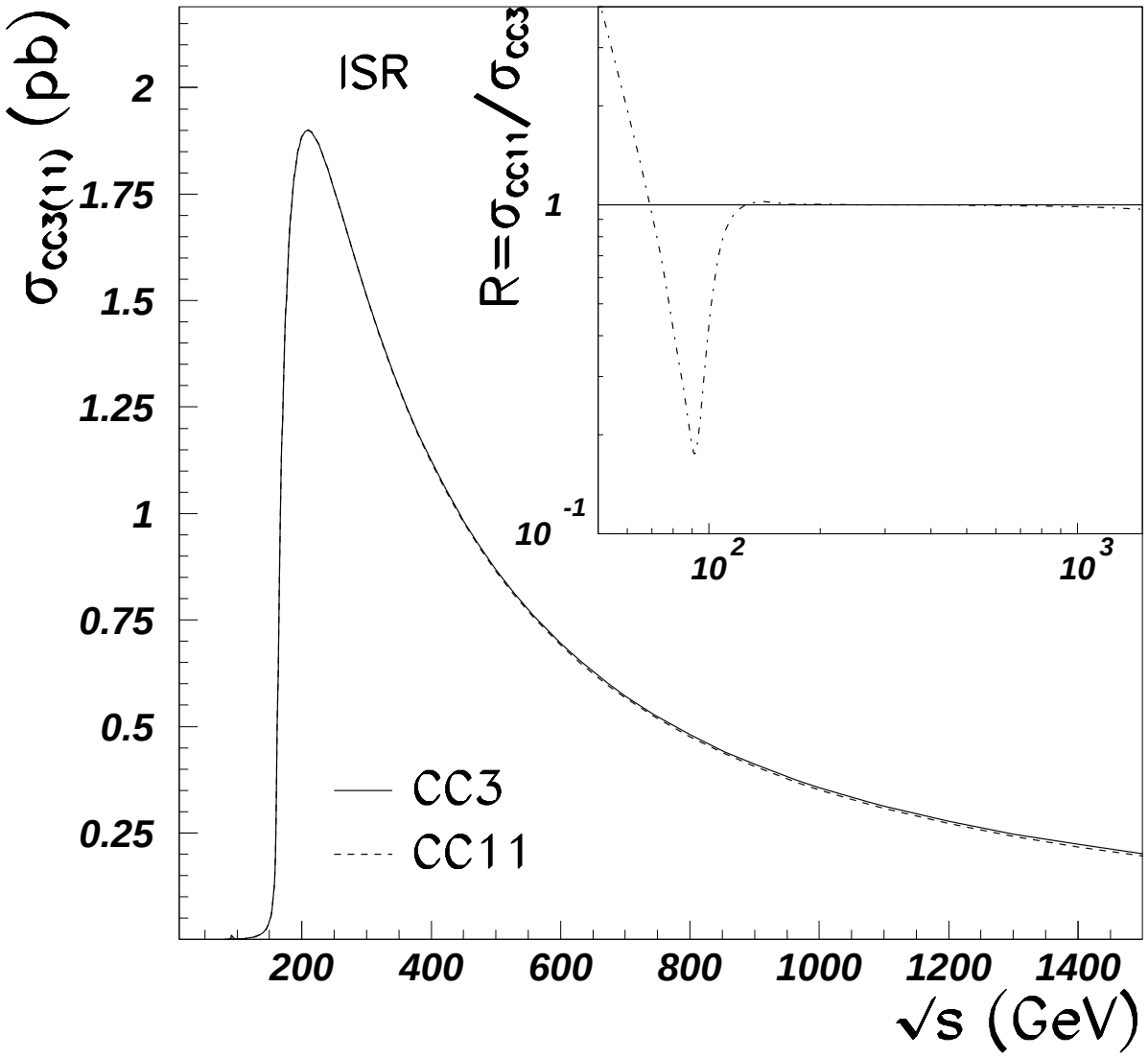

Figure 6: *The ratio of* `CC11` *and* `CC3` *processes with QED corrections.*

A Some properties of the auxiliary functions $\lambda(s, s_1, s_2)$ and $\mathcal{L}(s; s_1, s_2)$

Some of the properties of the two auxiliary functions λ and $\mathcal{L}$ are collected here. We begin with the λ function:

$$\begin{aligned}\lambda &\equiv \lambda(s, s_1, s_2) = \lambda(s_1, s, s_2) = \lambda(s_2, s_1, s) \\ &= s^2 + s_1^2 + s_2^2 - 2ss_1 - 2s_1s_2 - 2s_2s \\ &= \left[s - (\sqrt{s_1} + \sqrt{s_2})^2\right]\left[s - (\sqrt{s_1} - \sqrt{s_2})^2\right]. \end{aligned} \tag{A.1}$$

The λ function is symmetric in its arguments. From (A.1), the zeroes may be read off easily. One is the virtual threshold (and integration boundary),

$$\sqrt{s} = \sqrt{s_1} + \sqrt{s_2}, \tag{A.2}$$

the other one is unphysical. On the mass shell, the following limit holds:

$$\begin{aligned}\sqrt{\lambda(s, M_W^2, M_W^2)} &= s\beta(s, M_W^2), \\ \beta(s, M_W^2) &= \sqrt{1 - \frac{4M_W^2}{s}}. \end{aligned} \tag{A.3}$$

The logarithm $\mathcal{L}$ is defined as follows:

$$\begin{aligned}\mathcal{L}(s; s_1, s_2) &= \mathcal{L}(s; s_2, s_1) \\ &= \frac{1}{\sqrt{\lambda}} \ln \frac{s - s_1 - s_2 + \sqrt{\lambda}}{s - s_1 - s_2 - \sqrt{\lambda}}. \end{aligned} \tag{A.4}$$

This function is symmetric in the last two arguments. For vanishingly small invariant masses, it is:

$$\lim_{s_1, s_2 \to 0} \mathcal{L}(s; s_1, s_2) = \frac{1}{s} \ln \frac{s^2}{s_1 s_2}. \tag{A.5}$$

The other important limit is approached when λ vanishes, which corresponds to the virtual threshold kinematics:

$$\lim_{\lambda \to 0} \mathcal{L}(s; s_1, s_2) = \frac{2}{s - s_1 - s_2} + \ldots \tag{A.6}$$

In the on mass shell limit, the following simplification holds:

$$\mathcal{L}(s; M_W^2, M_W^2) = \frac{2}{s\beta} \ln \frac{1 + \beta}{1 - \beta}. \tag{A.7}$$

In the ultra-relativistic limit, i.e. when M_W^2 becomes vanishingly small compared to s, one better uses

$$\lim_{M_W^2/s \to 0} \mathcal{L}(s; M_W^2, M_W^2) = \frac{2}{s} \ln \frac{s}{M_W^2}. \tag{A.8}$$

B Four-momenta and phase space variables

In this appendix, we express the four-momenta k_i and p_j in terms of the variables, which are used for the parameterization of the phase space: $s_1, s_2, \theta, \theta_i, \phi_i$. Then, the phase space integration over the squared matrix elements, which are expressions in the scalar products $k_i k_j, k_i p_l, p_l p_n$, $i, j = 1, 2$, $l, n = 1, \ldots 4$, may be easily performed.

In the center of mass frame, the initial state vectors k_1 and k_2 are given by

$$k_1 = (k_0, \ -k\cos\theta, \ 0, \ k\cos\theta), \tag{B.1}$$
$$k_2 = (k_0, \ k\cos\theta, \ 0, \ -k\cos\theta), \tag{B.2}$$

with

$$k_0 = \frac{\sqrt{s}}{2}, \tag{B.3}$$
$$\left|\vec{k}_i\right| \equiv k = \frac{\sqrt{\lambda(s, m_e^2, m_e^2)}}{2\sqrt{s}}. \tag{B.4}$$

This allows to calculate $k_1 k_2$.

The products $p_1 p_2$ and $p_3 p_4$ may be determined in the rest systems of the corresponding fermion pairs. For the 'compound' V_1 (corresponding to the W^- boson in case of resonant production), the rest system R is defined by the condition

$$p_{12} = p_1 + p_2, \tag{B.5}$$
$$\vec{p}_{12}^{\,R} = 0. \tag{B.6}$$

It is

$$p_{1,0}^R = \frac{s_1 + m_1^2 - m_2^2}{2\sqrt{s_1}}, \tag{B.7}$$
$$p_{2,0}^R = \frac{s_1 - m_1^2 + m_2^2}{2\sqrt{s_1}}. \tag{B.8}$$

The 3-momenta of the two fermions are pointing into opposite directions and we have:

$$|\vec{p}_1^{\,R}| = |\vec{p}_2^{\,R}| \equiv p_{12}^R = \frac{\sqrt{\lambda(s_1, m_1^2, m_2^2)}}{2\sqrt{s_1}}. \tag{B.9}$$

The components of the fermion momenta p_1 and p_2 in the rest system of the fermion pair are ($p_i^R = \{p_{i,0}^R, p_{i,x}^R, p_{i,y}^R, p_{i,z}^R\}$, i=1,2):

$$p_1^R = \left\{p_{1,0}^R, p_{12}^R \sin\theta_1 \cos\phi_1, p_{12}^R \sin\theta_1 \sin\phi_1, p_{12}^R \cos\theta_1\right\}, \tag{B.10}$$
$$p_2^R = \left\{p_{2,0}^R, -p_{12}^R \sin\theta_1 \cos\phi_1, -p_{12}^R \sin\theta_1 \sin\phi_1, -p_{12}^R \cos\theta_1\right\}. \tag{B.11}$$

These relations allow the calculation of the product $p_1 p_2$ in terms of the integration variables; similar relations hold for the other fermion pair and the product $p_3 p_4$.

The remaining Lorentz invariant scalar products $k_i p_j, p_1 p_3$, etc., may be calculated by boosting all the final state momenta into the center of mass system. We will assume that

the 'compound' V_1 moves along the positive z axis. Then, it is in the center of mass system ($p_{34} = p_3 + p_4$):

$$p_{12,0} = \frac{s + s_1 - s_2}{2\sqrt{s}}, \tag{B.12}$$

$$p_{34,0} = \frac{s - s_1 + s_2}{2\sqrt{s}}, \tag{B.13}$$

$$|\vec{p}_{12}| = |\vec{p}_{34}| = \frac{\sqrt{\lambda}}{2\sqrt{s}}. \tag{B.14}$$

With the aid of the above definitions the Lorentz transformation from the center of mass system (and back) may be expressed. The components of p_1 transform from the rest system of V_1 into the center of mass system according to:

$$p_{1,0} = \gamma_{12}^0\, p_{1,0}^R + \gamma_{12}\, p_{1,z}^R, \tag{B.15}$$

$$p_{1,x} = p_{1,x}^R, \tag{B.16}$$

$$p_{1,y} = p_{1,y}^R, \tag{B.17}$$

$$p_{1,z} = \gamma_{12}\, p_{1,0}^R + \gamma_{12}^0\, p_{1,z}^R, \tag{B.18}$$

where

$$\gamma_{12}^0 \equiv \frac{p_{12,0}}{\sqrt{s_1}} = \frac{s + s_1 - s_2}{2\sqrt{s s_1}}, \tag{B.19}$$

$$\gamma_{12} \equiv \frac{|\vec{p}_{12}|}{\sqrt{s_1}} = \frac{\sqrt{\lambda}}{2\sqrt{s s_1}}, \tag{B.20}$$

and analogously for p_2 and for the other fermion pair. One should have in mind that for the 'compound' V_2 the sign of the transformation of the z component is negative.

As a result of all these relations, we may finally express the components of the four final state momenta in the center of mass system, $p_i = \{p_{i,0}, p_{i,x}, p_{i,y}, p_{i,z}\}$, $i = 1, \ldots 4$:

$$\begin{aligned}
p_1 &= \left\{\gamma_{12}^0 p_{1,0}^R + \gamma_{12} p_{12}^R \cos\theta_1,\ p_{12}^R \sin\theta_1 \cos\phi_1,\ p_{12}^R \sin\theta_1 \sin\phi_1,\ \gamma_{12}^0 p_{12}^R \cos\theta_1 + \gamma_{12} p_{1,0}^R\right\},\\
p_2 &= \left\{\gamma_{12}^0 p_{2,0}^R - \gamma_{12} p_{12}^R \cos\theta_1,\ -p_{12}^R \sin\theta_1 \cos\phi_1,\ -p_{12}^R \sin\theta_1 \sin\phi_1,\ -\gamma_{12}^0 p_{12}^R \cos\theta_1 + \gamma_{12} p_{2,0}^R\right\},\\
p_3 &= \left\{\gamma_{34}^0 p_{3,0}^R - \gamma_{34} p_{34}^R \cos\theta_2,\ p_{34}^R \sin\theta_2 \cos\phi_2,\ p_{34}^R \sin\theta_2 \sin\phi_2,\ \gamma_{34}^0 p_{34}^R \cos\theta_2 - \gamma_{34} p_{3,0}^R\right\},\\
p_4 &= \left\{\gamma_{34}^0 p_{4,0}^R + \gamma_{34} p_{34}^R \cos\theta_2,\ -p_{34}^R \sin\theta_2 \cos\phi_2,\ -p_{34}^R \sin\theta_2 \sin\phi_2,\ -\gamma_{34}^0 p_{34}^R \cos\theta_2 - \gamma_{34} p_{4,0}^R\right\}.
\end{aligned} \tag{B.21}$$

With these relations, any of the scalar products may be expressed in terms of integration variables. It may be seen explicitly that in the center of mass system the $(p_1 + p_2)$ and $(p_3 + p_4)$, as well as $(k_1 + k_2)$, are independent of all angular variables while $(p_1 - p_2)$ and $(p_3 - p_4)$, as well as $(k_1 - k_2)$, depend each on only one angle θ_1, θ_2, θ, respectively.

C Phase space integrals

The gauge boson propagators depend on one of the invariant masses squared s, s_1, s_2 and are left for numerical integrations. Thus, the only angular integrals will arise from fermion propagators. In this respect, the `CC3` process is distinguished by its simplicity since the final state integrations factorize completely and may be performed by tensor integration over θ_i, ϕ_i and then the neutrino propagator in the `crab` diagram contains the only nontrivial angular dependence:

$$D_\nu \;\sim\; \frac{4}{\left[(k_1-k_2)-(p_1+p_2)+(p_3+p_4)\right]^2} = \frac{2}{s-s_1-s_2-\sqrt{\lambda}\cos\theta} \equiv \frac{1}{t_\nu}. \qquad \text{(C.1)}$$

Here, only the difference $(k_1 - k_2)$ depends on an angle (see the final remarks in appendix B. The one dimensional integration is:

$$[A]_\theta \equiv \frac{1}{2}\int_{-1}^{+1} d\cos\theta \; A. \qquad \text{(C.2)}$$

Besides $[\cos^n\theta]_\theta = (1, 0, 1/3)$ for $n = 0, 1, 2$, the following integrals are used:

$$\left[\frac{1}{t_\nu}\right]_\theta \;=\; \mathcal{L}(s; s_1, s_2), \qquad \text{(C.3)}$$

$$\left[\frac{1}{t_\nu^2}\right]_\theta \;=\; \frac{1}{s_1 s_2}. \qquad \text{(C.4)}$$

The background contributions contain either one or two (equal or different) fermion propagators. An example is:

$$D_{f_1} \;\sim\; \frac{4}{\left[(k_1+k_2)-(p_1-p_2)+(p_3+p_4)\right]^2} = \frac{2}{s_1-s_2-s+\sqrt{\lambda}\cos\theta_1} \equiv \frac{1}{t_{f_1}}. \qquad \text{(C.5)}$$

which occurs in the second of the Feynman diagrams of figure 2. Here, only $(p_1 - p_2)$ depends on an angle. The other propagators are expressed similarly. Evidently, the angular integrations over ϕ_1, ϕ_2 are not influenced and those over $\theta, \theta_1, \theta_2$ factorize and may be performed independently using the above table of integrals, thereby permuting s, s_1, s_2 in the answers as needed. After a careful book-keeping, the background contributions are not much more involved than the `CC3` case.

D The neutral current kinematical functions

The off shell Z pair production may be described by one kinematical function [10]:

$$\mathcal{G}_{\texttt{NC2}}(s; s_1, s_2) \;=\; \frac{s^2 + (s_1+s_2)^2}{s - s_1 - s_2}\mathcal{L}(s, s_1, s_2) - 2. \qquad \text{(D.1)}$$

The process `NC24`, which proceeds via off shell gauge boson pairs, but also via single resonant diagrams of the `deer` type, may be described by two functions $\mathcal{G}_{\texttt{NC2}}$ and $\mathcal{G}_{\texttt{NC24}}$. The

latter is [5]:

$$\begin{aligned}\mathcal{G}_{\texttt{NC24}}(s;s_1,s_2) &= ss_1s_2\times\frac{3}{\lambda^2}\Bigg\{\mathcal{L}(s_2;s,s_1)\mathcal{L}(s_1;s_2,s)4s\Big[ss_1(s-s_1)^2+ss_2(s-s_2)^2\\ &\qquad +s_1s_2(s_1-s_2)^2\Big]\\ &\quad+(s+s_1+s_2)\Bigg[\mathcal{L}(s_2;s,s_1)2s\left[(s-s_2)^2+s_1(s-2s_1+s_2)\right]\\ &\qquad+\mathcal{L}(s_1;s_2,s)2s\left[(s-s_1)^2+s_2(s+s_1-2s_2)\right]\\ &\qquad+5s^2-4s(s_1+s_2)-(s_1-s_2)^2\Bigg]\Bigg\}. \qquad \text{(D.2)}\end{aligned}$$

The function $\mathcal{G}_{\texttt{NC24}}$ may be identified in the integrand on the right hand side of equation (2.11) in [31]. The quantity I_4, which is defined there and contains higher order axial corrections to the Z width, is related to $\mathcal{G}_{\texttt{NC24}}$ as follows:

$$I_4=\int\frac{ds_1ds_2}{s_1s_2}\frac{\sqrt{\lambda}}{3s}\mathcal{G}_{\texttt{NC24}}(s;s_1,s_2)=\frac{\pi^2}{3}-\frac{15}{4}. \qquad \text{(D.3)}$$

For numerical applications, the following limit is useful:

$$\lim_{\lambda\to0}\mathcal{G}_{\texttt{NC24}}(s;s_1,s_2) = \frac{1}{s_1s_2}\left[-\frac{9s^2-\Delta^2}{s^2-\Delta^2}-\frac{2}{3}\frac{\lambda}{(s^2-\Delta^2)^3}\left(9s^4+6s^2\Delta^2+\Delta^4\right)+\mathcal{O}(\lambda^2)\right], \qquad \text{(D.4)}$$

with $\Delta=s_1-s_2$.

References

[1] G. Altarelli (ed.), Proc. of the Workshop on Physics at LEP 2, CERN 1995, CERN Yellow Report in preparation.

[2] P. Zerwas (ed.), Proc. of the European Workshop on Physics with e^+e^- Linear Colliders, Annecy, Gran Sasso, Hamburg, 1995, in preparation.

[3] F.A. Berends, R. Kleiss and R. Pittau, Nucl. Phys. **B424** (1994) 308; Nucl. Phys. **B426** (1994) 344; Fortran program `EXCALIBUR`, *Comput. Phys. Commun.* **85** (1995) 437;
R. Pittau, *Phys. Letters* **B335** (1994) 490.

[4] D. Bardin, M. Bilenky, D. Lehner, A. Olchevski and T. Riemann, in: T. Riemann and J. Blümlein (eds.), Proc. of the Zeuthen Workshop on Elementary Particle Theory – Physics at LEP200 and Beyond, Teupitz, Germany, April 10–15, 1994, *Nucl. Phys.* (Proc. Suppl.) **37B** (1994) p. 148.

[5] D. Bardin, A. Leike and T. Riemann, *Phys. Letters* **B344** (1995) 383.

[6] D. Bardin, A. Leike and T. Riemann, *Phys. Letters* **B353** (1995) 513.

[7] E. Boos et al., `CompHEP`: computer system for calculation of particle collision characteristics at high energies, version 2.3 (1991), Moscow State Univ. preprint MGU-89-63/140 (1989); preprint KEK 92-47 (1992).

[8] J.A.M. Vermaseren, *Symbolic Manipulation with* `FORM`, Computer Algebra Nederland, Amsterdam, 1991.

[9] T. Muta, R. Najima and S. Wakaizumi, *Mod. Phys. Letters* **A1** (1986) 203.

[10] V. Baier, V. Fadin and V. Khoze, *Sov. Phys. JETP* **23** (1966) 104;
R.W. Brown and K.O. Mikaelian, *Phys. Rev.* **D19** (1979) 922;
M. Cvetic and P. Langacker, *Phys. Rev.* **D46** (1992) 4943; E: **D48** (1993) 4484.

[11] T. Sjostrand, Fortran programs `PYTHIA 5.7` and `JETSET 7.4` (Oct. 1994), *Comput. Phys. Commun.* **82** (1994) 74; updated version: Lund preprint LU TP 95–20 (1995) [hep-ph/9508391].

[12] D. Bardin et al., Report of the working groups on W pair production and Monte Carlo generators, in [1].

[13] G. Gounaris et al., Report of the working group on anomalous gauge boson couplings, in [1].

[14] A. Aeppli, preprint BNL-46819 (1991);
A. Aeppli and D. Wyler, *Phys. Letters* **B262** (1991) 125;
A. Aeppli, G.J. van Oldenborgh and D. Wyler, preprint PSI–PR–93–22;
G.J. van Oldenborgh, P.J. Franzini and A. Borrelli, *Comp. Phys. Commun.* **83** (1994) 14.

[15] F.A. Berends, G. Burgers and W.L. van Neerven, *Nucl. Phys.* **B329** (1990) 429; E: **B304** (1998) 921.

[16] B.A. Kniehl, M. Krawczyk, J.H. Kühn and R. Stuart, *Phys. Letters* **B209** (1988) 337.

[17] D. Bardin, M. Bilenky, A. Olchevski and T. Riemann, *Phys. Letters* **B308** (1993) 403; revised version: hep-ph/9507277, E: to appear.

[18] D. Bardin, D. Lehner and T. Riemann, in: Proc. of the IX Int. Workshop on High Energy Physics and Quantum Field Theory, Zvenigorod, Russia, Sept 1994, in press; preprint DESY 94–216 (1994) [hep-ph/9411321].

[19] D. Bardin, W. Beenakker and A. Denner, *Phys. Letters* **B317** (1993) 213;
see also: V.S. Fadin, V.A. Khoze and A.D. Martin, *Phys. Letters* **B311** (1993) 311; **B320** (1994)141; *Phys. Rev.* **D49** (1994) 2247.

[20] E.A. Kuraev and V.S. Fadin, *Sov. J. Nucl. Phys.* **41** (1985) 466.

[21] D. Bardin and T. Riemann, Fortran program `GENTLE`, version `CC11` (June 1995).
Version `CC11` originates from: D. Bardin, M. Bilenky, A. Olchevski and T. Riemann, Fortran program `GENTLE`: A semi-Monte Carlo `GEN`erator of the radiative `T`ail for `LE`P 200.

[22] A. Akhundov, D. Bardin and T. Riemann, *Nucl. Phys.* **B276** (1986) 1;
W. Beenakker and W. Hollik, *Z. Physik* **C40** (1988) 141;
J. Bernabeu, A. Pich and A. Santamaria, *Phys. Letters* **B200** (1988) 569;
see also: D. Bardin, W. Hollik and G. Passarino (eds.), Reports of the Working Group on Precision Calculations for the Z Resonance, CERN Yellow Report CERN 95–03 (1995).

[23] D. Bardin, S. Riemann and T. Riemann, *Z. Physik* **C32** (1986) 121;
F. Jegerlehner, *Z. Physik* **C32** (1986) 425; E: **38** (1988) 519;
A. Denner and T. Sack, *Z. Physik* **C46** (1990) 653.

[24] E. Accomando and A. Ballestrero, Fortran program `WPHACT`.

[25] G. Montagna, O. Nicrosini and F. Piccinini, Fortran program `WWGENPV`, A Monte Carlo Event Generator for Four-Fermion Production in $e^+e^- \to W^+W^- \to 4f$, preprint CERN-TH/95–100 (1995), to appear in *Comp. Physics Commun.*

[26] G. Passarino, Fortran program `WTO`.

[27] A. Leike, Contribution to the working group on Higgs boson physics of the Workshop [2].

[28] F. Berends and A.I. van Singhem, Leiden preprint INLO–PUB–7/95 [hep-ph/9506391]; see also [13].

[29] E.N. Argyres et al., preprint INLO–PUB–8/95 [hep-ph/9507216].

[30] D. Bardin, M. Bilenky, A. Olchevski and T. Riemann, preprint CERN-TH. 7102/93 (1993), in: P.M. Zerwas (ed.), Proc. of the Workshop on e^+e^- Collisions at 500 GeV: The Physics Potential, Munich, Annecy, Hamburg (Nov 1992 to April 1993), DESY 93-123C (1993) p. 159.

[31] B.A. Kniehl and J.H. Kühn, *Nucl. Phys.* **B329** (1990) 547.